

Final Report

and

Final Property Report

“Collaborative Proposal: Development of New Electronics, Repair and Testing Procedures for Very Broadband STS-1 Seismometers”

IRIS Subaward Agreement Number 387

June 14, 2007

**Thomas VanZandt
Metrozet, LLC
21143 Hawthorne Blvd., #456
Torrance, CA 90503
tom.vanzandt@metrozet.com**

I. Introduction

Under this subaward, Metrozet, LLC, in collaboration with the Berkeley Seismological Laboratory (BSL), has undertaken the development and test of new electronic hardware, and methods for mechanical repair, for the Streckeisen STS-1 Very Broad-Band (VBB) seismometer. The intent of this effort has been to develop simple and economical long-term solutions to current and anticipated problems with the existing STS-1 sensors. The primary aim was to develop a fully-tested, modern electronics module that is a drop-in replacement for the original electronics. A commercial product (the STS1-E300: see www.metrozet.com) has been developed. This module has been qualified by members of the GSN. This now provides users with a legitimate option for replacing old modules that are no longer functioning. This new electronics design addresses environmental packaging problems that have led to operational errors and failures in the existing instruments. This module also includes a set of electronic improvements that will make the installation and operation of the sensors more efficient. The system provides a fully-qualified calibration methodology that can be implemented easily by seismic technicians, using conventional recording systems. In addition to providing the potential for improved data quality within seismic networks using the STS-1, this new product offers greater flexibility with which the sensor can be installed and maintained. For example, these improved calibration methods allow individual STS-1 electronics modules to be switched between sensors, without loss of measurement accuracy. This is not currently possible, with the existing STS-1 instruments.

This final report summarizes work performed since the end of the last reporting period (December 31, 2006), and it identifies a number of future steps that Metrozet intends to pursue. Finally, we communicate a set of conclusions pertaining to the results for the entire program.

II. Results from Final Work Period

During this final work period, Metrozet has completed (or made significant progress) on the tasks set out as “Future Steps” in the last interim report. To summarize, the progress during this reporting period includes:

1. STS1-E300 Testing.

- a. **BSL Testing.** The commercial prototype STS1-E300 modules have been tested and optimized using the BSL sensor testbed. Both Metrozet and the BSL team have thoroughly exercised the modules. A number of minor modifications were implemented (relating to motor control functions and calibration stimulus amplitudes). Quiescent data was analyzed to ensure that the STS1-E300 modules were providing satisfactory transfer functions and equivalent or lower incoherent self-noise levels than those provided by the existing STS-1 electronics modules. The BSL testbed also allowed Metrozet to fabricate and test custom cabling used for later tests within the GSN network (at ASL and PFO, as discussed below).

Recently, BSL has moved a commercial prototype module to its Hopland, CA (HOPS) site. This replaces the three original feedback boxes used at this location. The internal calibration modes of the STS1-E300 will be used to determine, conclusively, whether the ongoing problems with these sensors are due to their electronics or their mechanical transducers.

- b. **Independent Evaluation by ASL.** Metrozet provided a set of custom cabling to support the integration of an STS1-E300 module with a triaxial set of STS-1 sensors at ASL (ANMO site), and with their Q680 data recorder. The module was thoroughly tested by ASL personnel (Bob Hutt and his team), who found the various operational modes of the module to be fully functional, as well as useful from a network operations standpoint.

The ASL deployment provided an initial opportunity to evaluate analog performance of the electronics in an ultra-low-noise environment (all previous testing had been conducted at BSL’s Byerly Vault). Metrozet and ASL agree that the new electronics are providing equivalent or better noise performance relative to the Streckeisen modules that they are replacing. The self-noise at high frequency (above 1 Hz) appears to be significantly improved (Bob Hutt, ASL, personal communication).

Metrozet has provided a detailed write-up on our noise test results. This is available at: <http://metrozet.com/Archive/ASL-STS1-E300-Analysis-5May07.pdf>. It is also attached in Appendix A. Comparative plots of Signal Power Spectral Density (PSD), Incoherent Noise PSD, and Coherence are shown in Figure 1. Of particular note is that the two sensors have nearly identical Signal PSDs at long period. This shows that the 360 second (nominal) corner frequency is maintained in the new electronics. In short, the transfer functions of the two sensors are very similar. The incoherent self-noise PSD of both sensors are well below the NLNM at all frequencies between 2 and 1000 seconds.

- c. **Independent Evaluation by UCSD IRIS/IDA Group at PFO.** Following testing at ASL, a commercial prototype module was moved to UCSD’s Pinyon Flat

Observatory (PFO) for independent evaluation by Peter Davis and his team. Metrozet provided custom cabling for connection of the STS1-E300 to UCSD's data recording system (SAIC digitizer). The module was installed on May 30, 2007. Already, we are seeing extremely low self-noise levels. Figure 2 shows the same comparative PSDs for data recorded at PFO. The incoherent noise of the STS-1 with Metrozet electronics is below the GSN Noise Model between 2.5 seconds and 800 seconds. Here, however, it is clear that the STS-1/Metrozet sensor has significantly lower self-noise than the PFO STS-1 reference sensor. Note that the lower coherence beyond 40 seconds is a result of the reference sensor noise. One can clearly see the effects of the reference sensor noise within the signal PSDs. A preliminary writeup of this data is attached in Appendix B.

PFO has a co-located STS-2 sensor which has been used to determine the high frequency response of the test sensor. Figure 3 shows a very good match between the reference (blue) and the STS-1/Metrozet sensor (test, in red) out to approximately 30 Hz. The Metrozet data has been de-convolved by a pair of conjugate poles (at $60.00 \pm 75.00j$ radians per second) in order to match the nominal response of the STS-2 sensor out to 30 Hz. Above 30 Hz, the lack of inter-sensor coherence renders further comparison meaningless. A preliminary writeup of this high frequency data is shown in Appendix C.

2. Calibration Software Tools

- a. **Scale Factor Calculator.** Metrozet has developed and tested a LabVIEW-based applet that reliably predicts the scalar responsivity of any STS-1 sensor that is mated with the new electronics. This applet ("Metrozet STS-1 Scale Factor Calculator V1.0"), whose graphical front panel is shown in Figure 4, requests user to enter the component values and response factors from the original STS-1 Factory Calibration Sheet. It then calculates the BRB (velocity) and LP (acceleration) scale factors for the same sensor with the STS1-E300 electronics. This applet has been used to calculate scale factors for the sensors during each of the above tests.

This applet has been tested at ASL and it predicted the new response to better than 1%. There is one caveat. The accuracy of the calculation assumes that the original factory scale factors are still accurate. This is obviously not the case with all STS-1 sensors in the world. Clearly, a method for verifying the scalar response of any STS-1 mechanical sensor will be needed in order to verify this assumption. While a number of techniques have been developed to perform this "absolute calibration" (including a step technique developed by Erhard Wielandt), Metrozet feels that ASL's proposed "STS-2 Transfer Standard Sensor" technique (Bob Hutt, personal communications) is the most practical. As part of scheduled maintenance of STS-1 sensor installations, a well-characterized STS-2 portable sensor can be co-located with the STS-1. This will allow a transfer standard measurement of the STS-1 scalar response (V/m/sec) in a very short time. This measurement can be made using either the new Metrozet electronics (best as it is a direct measurement) or with the old electronics (followed by use of the scale factor calculator).

Comparative Plots from ASL Data

Vertical STS-1 Sensors:

ASL Reference STS-1 with Factory Electronics (BLUE)

STS-1 with Metrozet STS1-E300 Electronics (RED)

NLNM (GREEN)

Using Q680 Digitizer LH data (1 Hz Output; 0.4 Hz Nyquist)

SIGNAL PSD

INCOHERENT NOISE PSD

COHERENCE

INCOHERENT NOISE PSD Calculated Assuming Identical Sensors

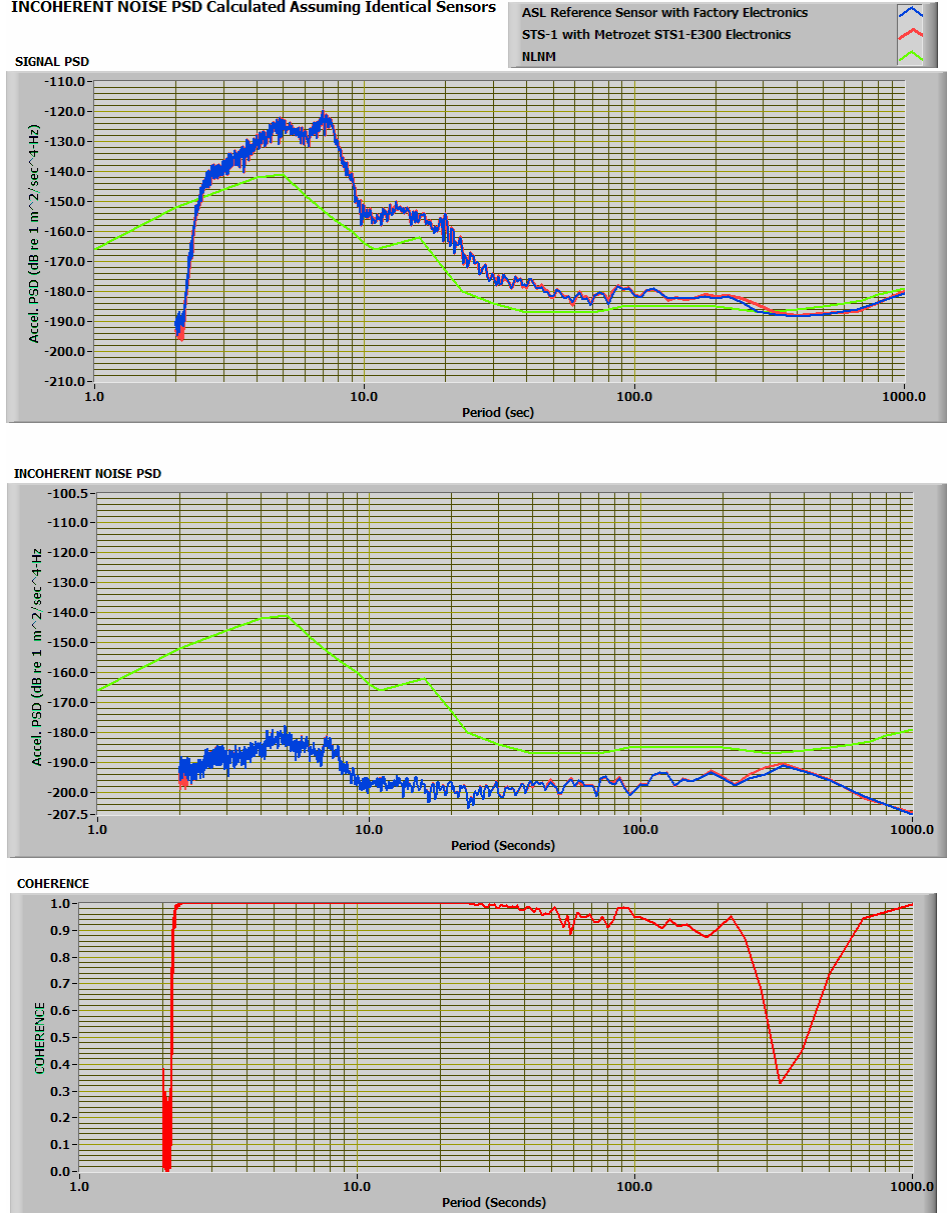


Figure 1. Data from ASL. Signal PSD, Incoherent Noise PSD, and Inter-sensor coherence plots from tests at PFO. Data from the PFO Reference Z STS-1 is shown in blue. Data from the Metrozet/Test sensor is shown in red. The NLNM is shown in green. The self-noise of an STS-1 with the Metrozet electronics is well below the NLNM over the entire analysis bandwidth (2.5 seconds to 1000 seconds).

Comparative Plots from pfo Data

Vertical STS-1 Sensors:

PFO Reference STS-1 with Factory Electronics (BLUE)

STS-1 with Metrozet STS1-E300 Electronics (RED)

GSN Noise Model (GREEN); after Berger, et al., JGR, 109, B11307 (2004)

Using SAIC Digitizer LH data (1 Hz Output; 0.4 Hz Nyquist)

SIGNAL PSD

INCOHERENT NOISE PSD

COHERENCE

INCOHERENT NOISE PSD Calculated Assuming Identical Sensors

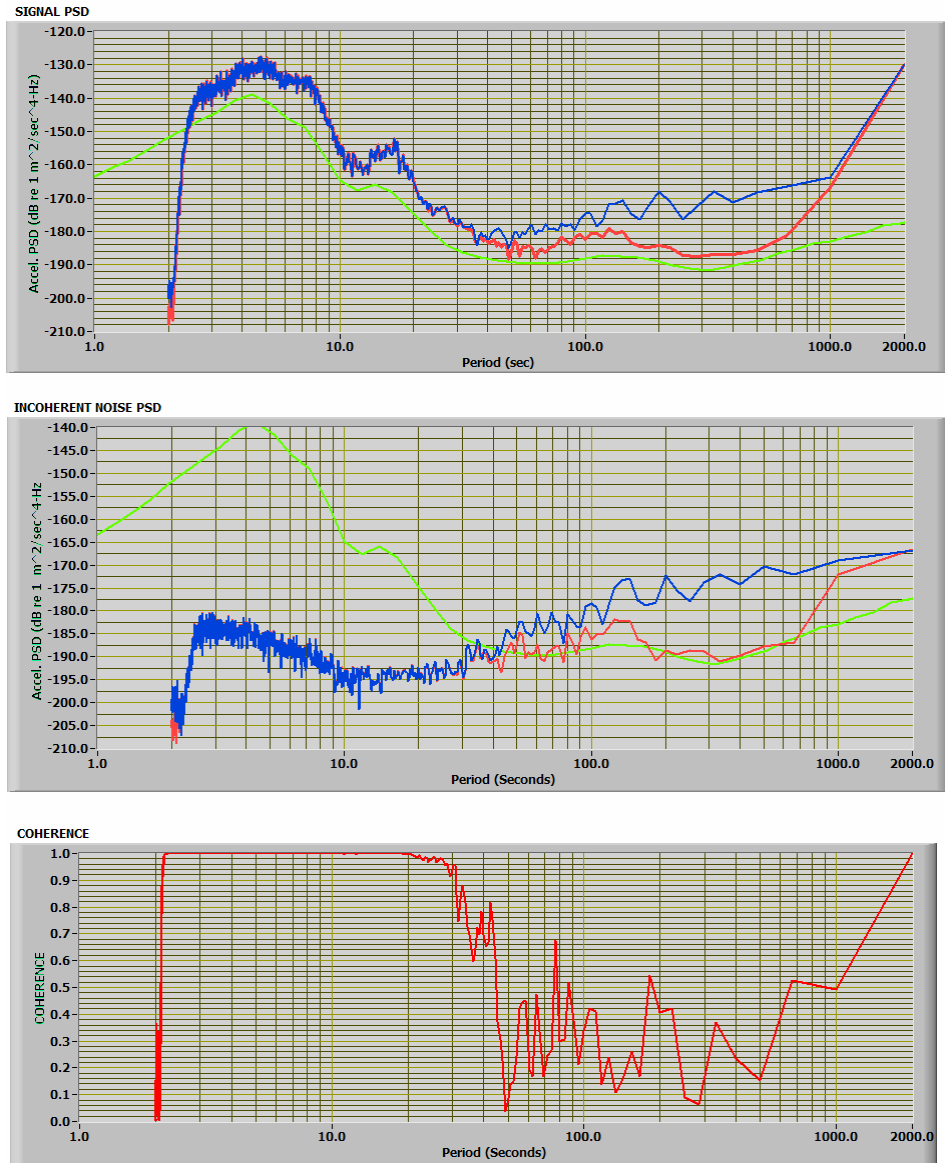


Figure 2. Data from PFO. Signal PSD, Incoherent Noise PSD, and Inter-sensor coherence plots from tests at PFO. Data from the PFO Reference Z STS-1 is shown in blue. Data from the Metrozet/Test sensor is shown in red. The PFO Reference sensor is clearly noisier. This causes the drop off in inter-sensor coherence beyond 40 seconds. The GSN Noise Model is shown in green.

Comparative Plots from 100 Hz PFO Data
Vertical Metrozet/STS-1 Sensor and PFO STS-2 Sensor:

PFO Reference STS-2 (BLUE)

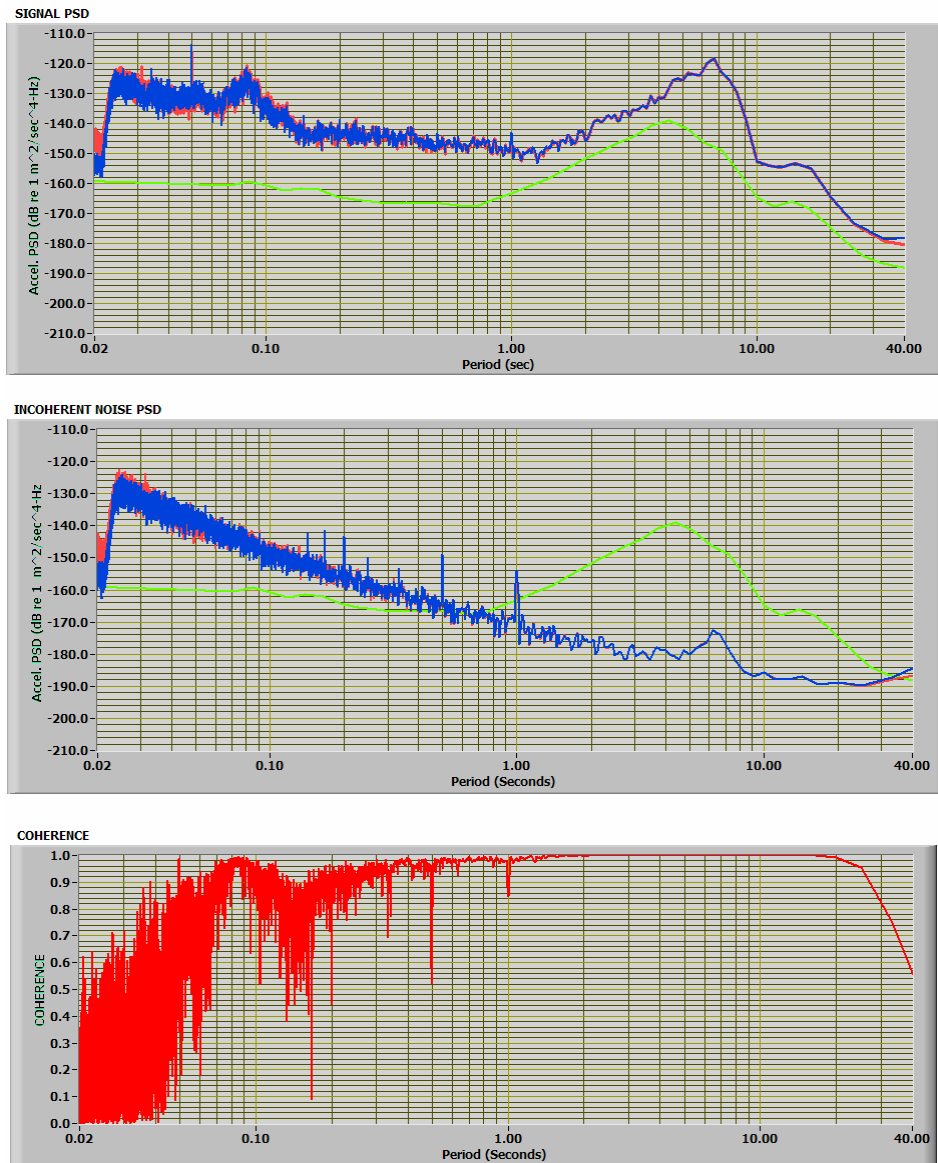
STS-1 with Metrozet STS1-E300 Electronics (RED)

GSN Noise Model (GREEN); after Berger, et al., JGR, 109, B11307 (2004)

Using SAIC Digitizer Data (100 Hz Output; 40 Hz Nyquist)

SIGNAL PSD
INCOHERENT NOISE PSD
COHERENCE

INCOHERENT NOISE PSD Calculated Assuming Identical Sensors



b. Figure 3. Data from PFO. Comparative High Frequency Data. Signal PSD, Incoherent Noise PSD and Inter-sensor coherence plots for 100 Hz data from PFO. PSD data from the STS-2 reference sensor is shown in blue. Data from the Metrozet/STS-1 test sensor is shown in red. The STS-1 data is de-convolved using a nominal pair of conjugate poles at $-222.14 \pm j222.14$ radians per second. The Metrozet/Test data is de-convolved using a pair of conjugate poles at $-60.00 \pm j75.00$ radians per second. Agreement is very good up to 30 Hz.

c.

Enter Data from Original STS-1 Calibration Sheet
Use Higher Value of R1 (e.g., if 412.6K/7392K, use 7392K)

Click "Enter and Continue" Button When Finished

Sensor Serial Number	R1 (ohms)	Single-Ended BRB Scale factor (V/m/sec)
38502	7000000	1203.00
	R2 (ohms)	Single-Ended LP Scale Factor (V/gal)
	1630	39.60
	R3 (ohms)	
	44070	
	C (F)	
	7.680E-6	
	RSI (ohms)	
	17737	
	RSII (ohms)	
	192	

Enter and Continue



Figure 4. Data Entry Screen from Metrozet STS-1 Scale Factor Calculator V1.0.

b. Frequency Response Analysis. The remote, automated calibration capability (internally-generated step/sweep signals, velocity and acceleration-equivalent stimuli, and auto-channel switching) provided by the STS1-E300 provides a powerful new tool for verifying sensor performance through frequent calibration. In the future there will be no reason not to perform periodic calibration within all major STS-1 sensor networks. Put another way, networks that are not performing regular calibrations will find it difficult to maintain high grades for data quality. The value of a remote calibration cannot be overstated. For example, almost immediately after installation of an STS1-E300 module at the BSL HOPS site, a remote calibration has verified that a long-held suspicion about the poor state-of-health of one (or more) of the STS-1 mechanical sensors. Calibration via the STS1-E300 module has shown that the high frequency response of the sensor is greatly limited. Note that this has not been observable in the past due to the severe limitations of the calibration hardware within the existing electronics (only acceleration-equivalent stimuli were available; this provides poor calibration at high frequency). It is expected that a much better understanding of the instantaneous state-of-health of the worldwide fleet of STS-1 sensors will be gained as these new modules are deployed. This will be an important driver for improved data quality.

The integrated calibration functions in the STS1-E300 are necessary, but not sufficient, tools. As mentioned in the previous progress report, Metrozet is adapting Professor Wielandt's CALEX5 (recursive time domain filter) analysis codes to a modern applet written in LabVIEW. This will analyze raw calibration data (in mini-SEED format) and generate frequency response factors (poles/zeros) for any sensor connected to the STS1-E300 electronics. During the final work period, Metrozet has implemented and tested an initial version (alpha) of this code. We will finish commercial development of this code in the last half of 2007. It is expected that this code will be distributed to any interested STS1-E300 customers.

- 3. Replacement Hinge Design.** Metrozet has identified a source (Avins Industrial Products/Matthey SA) of both die stamped, and chemically-etched, Phynox/Elgiloy. This will be used in both replacement hinge assemblies and within a proposed STS-1 replacement sensor (discussed below). The Phynox alloy (hardened grade with 280 KSI tensile strength and 260 KSI yield strength) is the original hinge material used in the STS-1. It is clear that modern thin gauge strip rolling techniques allow fabrication of suitable thin stock (0.0015" thickness), with extremely tight thickness tolerance (0.0001" to 0.0002" absolute, and under 0.0001" piece-to-piece). Precision forming of a final piece (either through mechanical stamping or photolithographic chemical etching) can be made to very high lateral accuracy. Although more expensive, etching may be preferred due to its ability to maintain superior flatness of the hinge strip. A number of useful features can be added during this forming process. A prototype design is shown in Figure 5. Here, the shim is notched in order to provide a positive stop, and azimuthal alignment, for more precise assembly of the strip into the hinge mount assembly. Also, a small hole aids in handling (holding) the shim. This will help to prevent damage to the hinge piece during assembly.

During this phase, Metrozet has contracted with an experienced micromechanical designer (Mr. Robert Calvet, P.E.) to perform an analysis of the current hinge design, and

to suggest improvements that can be made in a proposed replacement sensor. Mr Calvet has pointed out the contribution of the (arguably unnecessary) thinness, and (unintended) non-flatness of the hinge shims, to the very low side-load damage threshold in the STS-1 sensors. Basically, the hinge will be damaged (through a buckling mode displacement) when the moving boom is subjected to lateral accelerations in excess of 2 g. The need for a careful, pre-shipment clamping process is directly related to the inability of the STS-1 to tolerate lateral accelerations in excess of this. Two g is an unnecessarily small damage threshold. Mr Calvet's analysis indicates that re-designed hinge can be made that will allow lateral accelerations of between 10 and 20 gs before damage. This will allow shipment with a much simpler clamping mechanism, or even without clamping (The utility of an unclamped design has been demonstrated by Nanometrics in their Trillium sensor line.). The "expense" of a stronger hinge is very likely only a higher spring rate constant in the hinge. Note that the current hinge is already providing some restoring force and that an increase in this force is not expected to impose any performance limit to the design.

One point that has become clear during this program is that most users do not feel that the state-of-health of the mechanical sensors is a particularly large problem. The survey of STS-1 users conducted at the beginning of this program identified known problems with only about 5% of their installed axes (~25 out of 517 axes) Although the accuracy of this will become clear as new electronics modules are deployed (and routine calibrations are begun), it is not presently a significant, stated problem in the professional view of network operators. Although there may have been some reticence among the user community to discuss "problems" with their networks in a public setting, Metrozet's aggregate experience supports the conclusion that the business area of "STS-1 Repair Services" will not be a compelling one. While our understanding of specific (if limited) problems with the existing STS-1 mechanical sensors will be quite valuable as we embark on the development of an STS-1 replacement sensor, we frankly believe that there are other issues (namely improvements to packaging) that will be much more important in a replacement sensor.

Nevertheless, we have identified a source for precision fabricated hinge pieces, and we are willing to discuss this with any interested user.

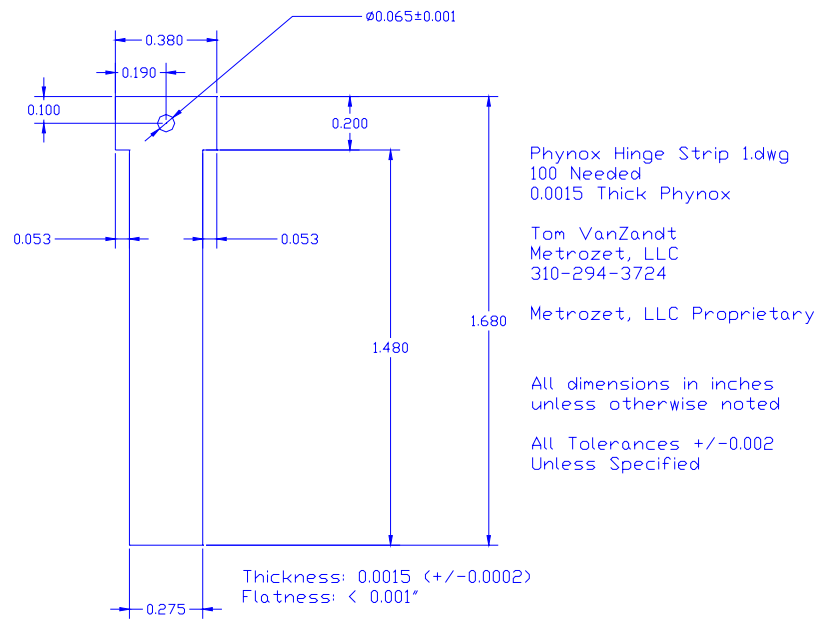


Figure 5. Mechanical Draawing of Precision-Formed Phynox Hinge Shim. The 0.275” portion of this 0.0015” thick piece replaces the standard shim. The notches at the top provide a positive stop within the STS-1 hinge mounting bars. The small hole allows handling of the shim without touching (damaging) its edges.

4. **Program deliverables to IRIS.** The main deliverables include:

- a. An STS1-E300 module. Per approval of IRIS, Metrozet will retain a number of commercial prototype modules as we begin to enter commercial production. Interested users wishing to test one of these module should contact us discuss the application and to make arrangements
- b. A set of electronic schematic design files. These are files that are compatible with the Orcad Unison Suite. There are separate files for both the mixed signal motherboard and the separate analog sensor modules.
- c. VHDL design file for programming a Complex Programmable Logic Device (CPLD) used within the motherboard.
- d. C code used to develop the firmware for the MSP430F169IPM microcontroller (Texas Instruments) used within the motherboard.
- e. Mechanical drawings (in AutoCAD LT 2004) for the modifications to the die-cast aluminum housing and for an aluminum plate used to mount the motherboard within the housing.
- f. LabVIEW (8.20) source code for “Metrozet STS-1 Scale Factor Calculator V1.0.vi”, and for all included subroutines (sub-VIs).
- g. Copies of the following documents:
 - i. Two interim progress reports
 - ii. This final report
 - iii. Current STS1-E300 data sheet
 - iv. Current STS1-E300 User’s Manual

All of the documents (items b-g) will be provided in electronic form.

III. Future Steps

As mentioned above, the STS1-E300 electronic module is now commercially available. Metrozet is accepting orders for this product. We expect to work with initial customers within the GSN to develop a common approach for cabling. Once this is developed, Metrozet will initiate a volume build for the cables at its preferred cable manufacturer. This should provide the highest reliability and value for customers of the STS1-E300.

Pre-shipment testing of the STS1-E300 will involve the use of both a comprehensive, PC-based, diagnostic test fixture being developed by Metrozet, and the evaluation of analog performance (noise and frequency response) on an actual triaxial set of STS-1 sensors. The former is to ensure satisfactory performance of all operating modes of the electronics. The latter is consistent with Metrozet’s goal of noise testing each sensor product that we deliver. The location of this “live testing” is still to be determined (and negotiated), however, it very likely will occur at one of the GSN customers.

Per discussions with personnel at BSL, ASL, and UCSD, Metrozet will finalize the design for an external power and telemetry module (the STS1-PTM1). This module will integrate a commercial DC-DC converter (for conversion between unregulated 9-36V and the regulated +/- 15V required by the STS1-E300), an RS-232-to-USB converter, an RS-232-to-ethernet converter, and power fusing. This external module will provide bulkhead 9-pin D (for RS-232), USB-A (for USB), and RJ-45 (for Ethernet) connectors. It will provide dedicated connectors for the analog control output lines, and auxiliary analog and digital input lines. The STS1-PTM1 will connect to the STS1-E300 via the CONTROL cable. Note that some users (e.g., UCSD) will probably not require this module for use within their existing systems.

Metrozet is committed to finishing commercial development of the frequency response analysis tool (based upon CALEX 5). It will be launched later this year as an executable LabVIEW applet: CALEX-EW.

Most importantly, Metrozet will team with UC Berkeley (BSL) and Professor Erhard Wielandt on a follow-on proposal that will develop a manufacturable, STS-1-grade replacement mechanical sensor. This work will seek to maintain the successful relationship (and high throughput test methodology) that was demonstrated during this program. The new proposal will seek to involve ASL on a more formal basis (as a development testing and evaluation partner), via a US Government Cooperative Research and Development Agreement (CRADA).

The proposed sensor will be compatible with the STS1-E300 electronics module. It will be a quasi-transportable, triaxial sensor which is far more integrated than the current STS-1 sensors. It will incorporate a number of valuable, new features, including capacitive position sensing (for lower noise at high frequency), on-board feedback trimming (ensuring closely matched response for all sensors with any STS1-E300 module), and a higher upper corner frequency (20 Hz or above). The proposed sensor will, however, maintain the specific design features that make the STS-1's performance unique. ***Metrozet's expectation is that the new sensor will provide STS-1 level performance at a cost that is competitive with currently-available, lower-performance, transportable sensors.***

The team has discussed the proposed work with both IRIS and the National Science Foundation (NSF). We have received and incorporated valuable feedback from both organizations. These discussions involved the perceived need for such a development (high), the availability (and sources) for the required funding, the expected program duration, and the compelling opportunity for training and educating the next generation of seismic sensor engineers and scientists. The team will submit a proposal to NSF (EAR/IF program) by July 11, 2007.

IV. Conclusions

This work has led to many technical improvements and developments that promise to improve the operation and maintenance of the worldwide STS-1 sensor fleet. Many of these have already been discussed in this and past reports. At the completion of this program, Metrozet feels that it is important to communicate three high-level points.

1. **Functionality.** The greatly increased functionality provided by the STS1-E300 (including remote control of sensor parameters, automated motor control, automated calibration, and comprehensive system diagnostics) should enable a new level of operability of seismic sensors within a network. The ability of a fully remote-controlled sensor to eliminate the need for a single remote site visit can save thousands of dollars for

network maintenance staffs. The ability to perform rapid calibrations (with the proper stimulus signal conditioning) should lead to a new level of quality assurance. At risk of overstating the case, it is fairly clear that all future VBB sensors will need to evolve in order to provide these capabilities. Those that do not (or those networks that do not use them) will simply be at a competitive disadvantage.

While we applaud any efforts at automating the operation of the seismic networks, Metrozet feels that the “data-recorder-centric” view of this automation is severely limited. No data recorder will be able to access and control all of the signals and features of a particular sensor. The simple proof of this is that the complete feature set available in the STS1-E300 is not available via any of the existing commercial recording systems, despite the fact that they have had many years to implement them. In fact, to the best of our knowledge, no recorder implements a single-step autocenter for the STS-1, no recorder provides acceleration and velocity-equivalent calibration stimuli for the STS-1 sensor (with the exact signal levels needed), and no recorder provides automated output signal switching to allow triaxial sensor calibration within a three channel recorder. Although these are all possible in principle, it is simply too complex and costly to implement, test, and support all of these features in any one recorder. It is clear that providing these (and other) capabilities within the sensor itself is a more reasonable proposition.

2. Myths. Many outside of IRIS/NSF have held the view that best-in-class VBB sensors or sensor electronics could only be developed by one or two small (non-US) companies has been de-bunked. Specifically, Metrozet was told, both before and during this program, by a number of seismic instrumentation “experts”, that it is simply too difficult to design and test STS-1 electronics. The strong suggestion was that this work would not be successful and that the money should not be invested. Note that very few (if any) specific technical arguments were proffered to support this view. No one could (or would) explain why this sort of development is beyond the range of experienced instrumentation physicists and engineers (e.g., the BSL/Metrozet/Wielandt team). What “arguments” that were made were weak at best. “You cannot buy good enough capacitors/resistors/amplifiers anymore,” was one. “Testing takes too long,” was another argument. In fact, one can procure higher quality passive components today, the original amplifiers are all still available (albeit in modern packages), and a robust, daily experimental testing routine can be used to successfully develop and test the sensors.

The point here is not about settling scores, but about the danger of imposing vague limitations on the seismic community, and its commercial suppliers. Note that as the team moves forward (hopefully) with an STS-1 replacement sensor development program, a new set of objections may be raised. We have heard some of them already: “the hinge material is no longer available,” “no manufacturer will provide the small quantities of compensated spring material that you will use,” and the general caution that “the sensor is not manufacturable,” are some of the common ones. The responses, respectively, are: Phynox is readily available with very tight mechanical tolerances, NiSpanC (or equivalent compensated spring metals) are available for nominal lot charges, again to very tight tolerances, and the field of precision manufacturing has evolved considerably since the time (late 1970s and early 1980s) that the STS-1 was developed. If one looks carefully at the components within an STS-1 sensor, they will

find that nearly everything can be manufactured today, to much tighter tolerances, at much lower cost. To be honest, it is an exciting time to be working in this area. Improved design and manufacturing tools allow innovative suppliers, such as Metrozet, to manufacture provide high performance products that are both reliable and cost effective. It is important for the seismic community to embrace and encourage these new developments, rather than dismissing them. The team thanks IRIS and the NSF for their foresight in this area.

3. Markets. As new VBB sensor products are proposed, developed, and qualified, the seismic community's self-identified need for a replacement for the STS-1 (the "How will we replace the STS-1?" question that has been a topic of numerous meetings and workshops) will be tested. Note that as entities such as BSL and Metrozet are stepping up to the challenge, the availability of development funding is one very good sign. Of greater importance, however, will be actual purchase orders.

The fact that STS-1 instruments could no longer be purchased or repaired led some in the community to (pragmatically) question whether the STS-1 is really needed at all. Unfortunately, the community has always viewed the STS-1 as a highly-specialized instrument: one that is much more expensive, much harder to install, and thus, suitable for only a limited number of deployments. While probably correct for the Streckeisen version of the instrument (with high cost, antiquated packaging, very long lead times, and difficult repair options), it is a mistake to maintain this mindset into the future. Quite simply, it arbitrarily segments the market (only this type of sensor for this, and only another for that) and it creates a disincentive for companies to develop products to serve it. In truth, a stable, long-term product with STS-1 level performance will be best developed and supported by a supplier who is also able to sell their products into the (larger) transportable sensor market. While Metrozet feels strongly that future STS-1 replacement sensors can be made much more transportable, and that they can be cost competitive with current transportable sensors, the community will need to be receptive to the idea that these sensors can be very useful in non-vault applications. Just as it makes sense to encourage transportable sensor manufacturers to improve their long period performance, it makes equal sense to encourage long-period sensor suppliers to attempt to package their sensors for larger volume applications. We applaud efforts by IRIS (including Rhett Butler and Kent Anderson) to push from both directions, and we encourage other stakeholders to do so as well. A major hope is that all procurements be open, transparent, and competitive, and that they have specifications that are dictated only by what is required technically. Without question, many past procurements within the community have been driven by what was felt to be available, what is normally used in this application, or what was favored by the purchasing organization. We hope that seismologists realize that a fully-competitive procurement process is essential for future commercial innovation.

Final Property Report

As of June 14, 2007 Metrozet, has acquired the following equipment for use on this task:

1. HP Media Center PC
Serial Number: MXF538038Y
and
Hyundai L72S LCD Monitor
Serial Number: L72SSBS35BK02488
Purchased in January, 2006
Purchase Price \$850
2. National Instruments PCI-6036E Data Acquisition Card
Serial Number: 0x1113060
Purchased in February, 2006
Purchase Price: \$1150
3. BK Precision 810C Capacitance Meter
Serial Number: 37006050064
Purchased in April, 2006
Purchase Price: \$150

Appendix A: Analysis of ASL Data

Analysis of STS1-E300 Measurements at Albuquerque Seismic Lab

Tom VanZandt, Metrozet, LLC

May 5, 2007

On April 4, 2007 Metrozet's STS1-E300 Electronics Module was installed on to a triaxial set of STS-1 sensors (2 Horizontal and 1 Vertical) at the USGS Albuquerque Seismological Laboratory (USGS/ASL, where GSN station ANMO is located). These sensors were co-located and co-aligned with ASL's permanent set of triaxial, STS-1 reference sensors. The reference sensors were operating using the original Streckeisen "Feedback Electronics" boxes. Signals from the six axes are being recorded using a Quanterra Q680 digitizer.

This experimental setup is being used by ASL personnel as part of an independent test of the Metrozet STS1-E300 electronics. The ASL team has been exercising the many operating modes of the STS1-E300 module (including its comprehensive sensor control, motor control, calibration, and diagnostic modes; see www.metrozet.com for details of the STS1-E300 module). One important test is to determine instrumental noise performance at a relatively quiet test site, such as ANMO. As is widely agreed, analysis of Z-axis (vertical) data is preferred in order to understand the noise contribution from the sensor electronics. This is because of the ability to measure background ambient seismic, as well as incoherent sensor noise, to much lower levels, using vertical sensors.

This analysis has been performed by Metrozet. However, careful attention has been paid ensuring that the spectral amplitudes agree closely with those calculated by Bob Hutt at ASL.

The data presented here are from a quiescent 16,000 second period (beginning on UTC day 105, at UTC time 08:49:49). 1 Hz (0.4 Hz Nyquist) data are used. The two raw data files used are available for download at www.metrozet.com.

The first:

"DATA_XX_NHYX_00_LHZ_2007_105_08_49"
is for the ASL reference STS-1 Z-channel (with factory electronics).

The second:

"DATA_XX_NHYX_20_LHZ_2007_105_08_49"
is for the test STS-1 Z-channel (with Metrozet STS1-E300 electronics)

The data are analyzed according to the following algorithm:

1. Raw data (counts) are multiplied by the digitizer scale factor. For the LH data, this value is $9.536E-7$ Volts per count (including the standard $2.384\mu\text{V}/\text{count}$ weight of the digitizer, and a 4X factor introduced by the Q680's LH, 1 Hz, decimation filter). Following this scaling, the data are in Volts.

2. The voltage data are divided by the scalar responsivity (2452 V-sec/m for the reference sensor, and 3336 V-sec/m for the test sensor). Note that the test sensor responsivity (using the STS1-E300) was calculated from the original factory calibration sheet, using “Metrozet STS-1 Scale Factor Calculator V1.0” software applet. As is shown below, this provides a nearly exact value for the scalar responsivity. Following this scaling, the data are in units of velocity (m/sec).
3. The data set is divided into 16 contiguous, non-overlapping segments, each of 1000 second length. There are two such sets of data: one for the reference sensor and one for the test sensor.
4. This data are windowed, using a Hanning window.
5. The power spectral density (PSD), and the inter-sensor coherence is calculated for each of the 1000 second records.
6. The PSD values are scaled to correct for the noise bandwidth factor of the Hanning window.
7. The PSDs and coherence records are stacked and averaged. The PSDs use RMS averaging and the coherence uses vector averaging. The result of this are two PSD spectra (SIGNAL spectra; one for each sensor), and a single coherence spectrum.
8. The SIGNAL PSD plots indicate that the long period response of the two sensors is nearly identical. As such, we apply a *nominal* long period de-convolution to the data (using a conjugate pole pair at $0.01234 \pm 0.01234i$ radians per second). This converts the PSD plots to “exact” velocity, over the band of 2.5 seconds to 1000 seconds. Note that at periods shorter than 2.5 seconds, the indicated velocity is affected by the Q680 decimation filter.
9. Using a standard algorithm for incoherent noise calculation (e.g., Barzilai, et. al., *Review of Scientific Instruments*, **69**, 2767 (1998)), we calculate the incoherent noise, that is attributable equally to each of the sensors. As is obvious from the data, this “identical” sensor treatment is quite justified: the signal PSD’s are identical, even within the frequency range exhibiting the lowest signal PSD values (50 to 1000 seconds).
10. All of the spectral data (SIGNAL PSD and INCOHERENT NOISE PSD) are converted to acceleration units, as is customary for this community. This is accomplished through spectral differentiation (multiplication by $2\pi f$ at each point). The resulting data are plotted in db units (re $1 \text{ mRMS}^2/\text{sec}^4\text{-Hz}$)
11. The resulting spectral plots do exhibit a degree of statistical variation (“noise”) in their values that is consistent with using only 16 averages. We do not perform any smoothing of these curves.

The resulting plots are shown below. The top plot shows the SIGNAL PSD. This is simply the background signal at ANMO. The overlap of the curves from the two sensors is nearly exact (typically to within 0.1 dB) over the entire band. The largest deviation occurs at periods at which the PSD values are the smallest (300 to 700 seconds). This is consistent with the fact that we are observing signal levels that are within 6 to 10 dB of the incoherent noise floor of the sensors. We expect, and observe, fluctuations between the recorded PSDs, due to the contribution of this incoherent noise. Note that with some data sets, the test data may have lower PSD values than the reference in this band. In others, the situation may be reversed (according to ASL analyses). For reference, the New Low Noise Model (NLNM) is plotted (green curve).

The second plot shows the INCOHERENT NOISE PSD for each sensor (using the other as a reference within the coherence calculation). Again, the noise plots overlap very closely. They are

well below the NLNM at all periods within this band. Note that the rise in calculated INCOHERENT NOISE within the microseismic noise band (2.5 to 10 seconds in this case) is not illustrative of the actual noise of either sensor. It is simply a consequence of the limitation of a coherence analysis to measure noise in the presence of large backgrounds. The practical limit to coherence is observed to be 0.999998 in this band. Given that the SIGNAL PSD levels approach -120 dB, coherence techniques can only be expected to resolve incoherent noise down to a level of -180 dB. ***We are quite certain that the actual INCOHERENT NOISE level of either sensor is at or below -200 dB within the microseismic band.***

The third plot shows the inter-sensor coherence. As discussed above, it is nearly 1.00000 within the microseismic band. As expected, it drops somewhat between 300-700 seconds. This is the point at which the ANMO background signal is dropping to a level that is close to the self-noise of each sensor.

In conclusion:

1. The STS1-E300 provides analog performance that is nearly identical to that of the original Factory Electronics box.
2. The calculated self noise of an STS1-E300-equipped sensor is well below the NLNM over the entire band used within this analysis (2.5 seconds to 1000 seconds).
3. The long period frequency response of a sensor using the STS1-E300 is indistinguishable to that of the original sensor.
4. The exact scalar responsivity of any STS-1 sensor using the STS1-E300 module can be calculated accurately, using a Metrozet-supplied software applet.

For Further Information

To discuss any details of this analysis, or of the STS1-E300 module, contact:

Tom VanZandt
Metrozet, LLC
1-310-294-3724
tom.vanzandt@metrozet.com

To discuss any details or observations regarding ASL's independent tests, contact:

Bob Hutt
ASL/USGS
1-505-846-5649
bhutt@usgs.gov

Comparative Plots from ASL Data
Vertical STS-1 Sensors:

ASL Reference STS-1 with Factory Electronics (BLUE)

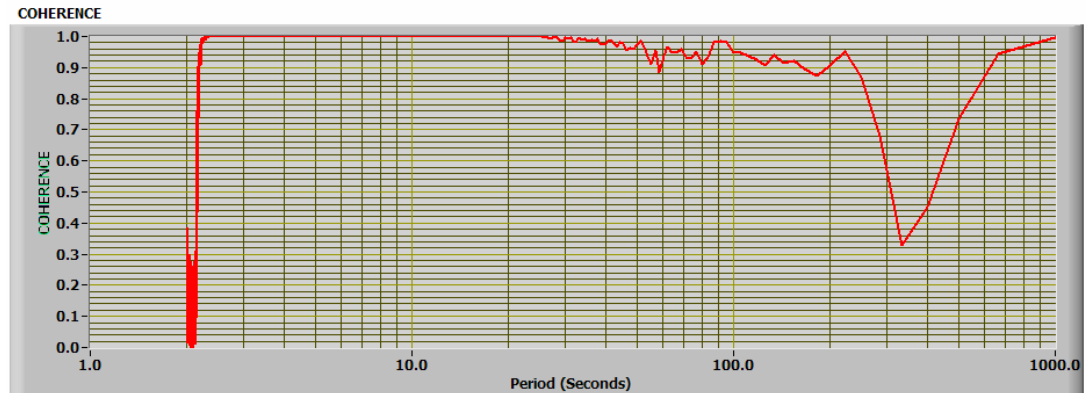
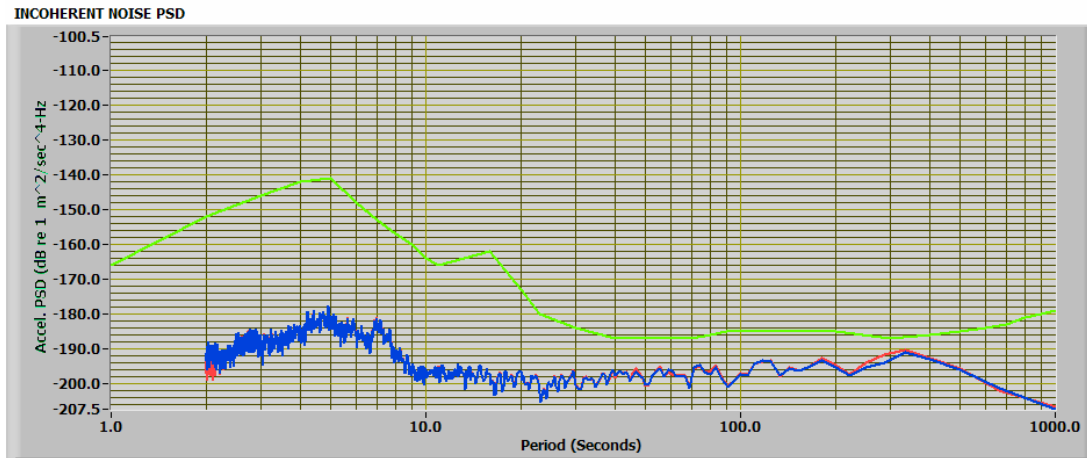
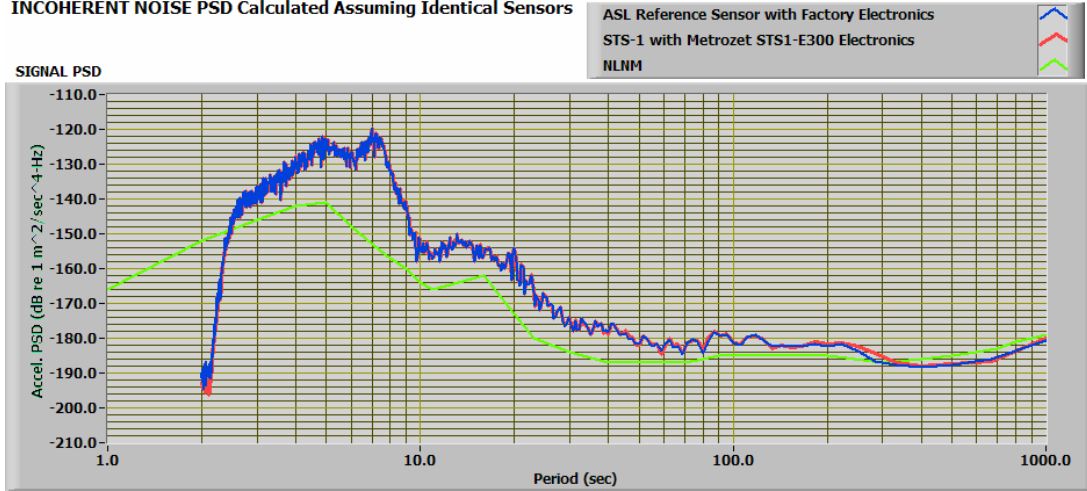
STS-1 with Metrozet STS1-E300 Electronics (RED)

NLNM (GREEN)

Using Q680 Digitizer LH data (1 Hz Output; 0.4 Hz Nyquist)

SIGNAL PSD
INCOHERENT NOISE PSD
COHERENCE

INCOHERENT NOISE PSD Calculated Assuming Identical Sensors



Appendix B: Analysis of PFO Long Period Data

Initial Analysis of Data from STS1-E300 Module Installed at PFO

Analysis provided by Metrozet, LLC

Tom VanZandt

June 14, 2007

On May 30, 2007 Metrozet and the IRIS/IDA team at UCSD installed an STS1-E300 electronics module at the Pinyon Flats Observatory (PFO). This is part of a continuing series of tests of the new electronics among members of the GSN (including Berkeley Seismographic Network, BSL, Albuquerque Seismic Lab, ASL, and UCSD).

The Metrozet electronics were connected to a triaxial set (E/N/Z) of STS-1 sensors. These “test” sensors were housed in one room of the PFO seismic vault. A permanent set of “reference” sensors is installed in an adjacent room of the vault.

Data presented here are from a 16,000 second quiet period. We have analyzed the LH data (1 Hz data rate, 0.4 Hz effective bandwidth). As is widely agreed, analysis of Z-axis (vertical) data is preferred in order to understand the noise contribution from the sensor electronics. This is because of the ability to measure background ambient seismic, as well as incoherent sensor noise, to much lower levels, using vertical sensors.

The exact calibration of the test Z mechanical sensor was unknown. The original “Factory Calibration Sheet” was not available at the time of these tests. As a result, we were unable to use “Metrozet’s STS-1 Scale Factor Calculator V1.0” to predict the exact scalar responsivity of the Z sensor mated with the Metrozet electronics. Within this analysis, we are determining the test sensor amplitude response empirically, using the known calibration of the reference STS-1 sensors. The calculated, mid-band scale factor for the STS-1/Metrozet sensor is 4817 V/m/sec, assuming that the PFO Test Z sensor has a scale factor of 2471 V/m/sec. This is consistent with the observed phenomenon of STS-1 vertical sensors exhibiting increased scale factors when connected to this version of the STS1-E300 (horizontal sensors exhibit scale factors slightly lower than the 2400 V/m/sec nominal).

The data are analyzed according to the following algorithm:

12. Raw data (counts) are multiplied by the digitizer scale factor. For the LH data, this value is $2.469E-7$ Volts per count. Following this scaling, the data are in Volts.
13. The voltage data are divided by the scalar responsivity (2471 V-sec/m for the reference sensor, and 4817 V-sec/m for the test sensor). Following this scaling, the data are in units of velocity (m/sec).
14. The data are de-meanned to remove the DC offsets.

June 14, 2007

Page20 of 26

15. The data set is divided into 8 contiguous, non-overlapping segments, each of 2000 second length. There are two such sets of data: one for the reference sensor and one for the test sensor.
16. This data are windowed, using a Hanning window.
17. The power spectral density (PSD), and the inter-sensor coherence is calculated for each of the 2000 second records.
18. The PSD values are scaled to correct for the noise bandwidth factor of the Hanning window.
19. The PSDs and coherence records are stacked and averaged. The PSDs use RMS averaging and the coherence uses vector averaging. The result of this are two PSD spectra (SIGNAL spectra; one for each sensor), and a single coherence spectrum.
20. We apply a *nominal* long period de-convolution to the data (using a conjugate pole pair at $0.01234 \pm 0.01234i$ radians per second). This converts the PSD plots to “exact” velocity, over the band of 2.5 seconds to 2000 seconds. Note that at periods shorter than 2.5 seconds, the indicated velocity is affected by the digitizer’s decimation filter.
The notional equivalency of the low frequency corners appears to be correct when one looks at the comparative long period time series (plotted below). If there were differences in, for example, long-period corner frequencies, then neither the amplitude, nor the phase, would agree over the 16000 second time series length. They do, in fact agree. As will be discussed below, the signal PSD values are significantly different at long period. The STS-1/Metrozet Test sensor records significantly lower signals (and has significantly lower self-noise) than that of the reference sensor. This difference can be as much as 20 dB. This is very clearly NOT due to some diminished response of the STS-1/Metrozet Test sensor. As discussed below, the reason for these differences is the very low background signal levels at PFO, and a higher self-noise in the reference sensor.
21. Using a standard algorithm for incoherent noise calculation (e.g., Barzilai, et. al., *Review of Scientific Instruments*, **69**, 2767 (1998)), we calculate the incoherent noise, that is attributable equally to each of the sensors. As is obvious from the data, this “identical” sensor treatment is not completely justified: the noise PSD’s not identical at the very low signal levels at PFO. However, this “identical” treatment is conservative, and the differences between it and alternative scenarios (all of the noise in the reference sensor, for example) will not change the data significantly at long periods (in that the coherence is low there).
22. All of the spectral data (SIGNAL PSD and INCOHERENT NOISE PSD) are converted to acceleration units, as is customary for this community. This is accomplished through spectral differentiation (multiplication by $2\pi f$ at each point). The resulting data are plotted in db units (re $1 \text{ mRMS}^2/\text{sec}^4\text{-Hz}$)
23. The resulting spectral plots do exhibit a degree of statistical variation (“noise”) in their values that is consistent with using only 8 averages. We do not perform any smoothing of these curves.

The resulting plots are shown below. The top plot shows the SIGNAL PSD. This is the background signal at PFO, plus sensor noise. The overlap of the curves from the two sensors is nearly exact (typically to within 0.1 dB) between 2.5 seconds and 40 seconds. Below 40 seconds the “signal” from the PFO reference Z sensor becomes significantly higher. We are clearly seeing noise in the reference sensor beyond 40 seconds. The PFO reference STS-1 Z sensor (or installation) is significantly noisier than the test sensor.

For reference, the GSN Noise Model (after Berger, et al, JGR, **109**, B11307 (2004)) is also plotted (green curve).

The second plot shows the INCOHERENT NOISE PSD for each sensor (using the other as a reference within the coherence calculation). Again, the noise plots overlap very closely to about 40 seconds. ***The Metrozet test sensor is at or below the GSN Noise Model at all periods between 2.5 and 800 seconds.*** Note that the STS-1/Metrozet Test sensor exhibits significantly lower self-noise than that of the Reference sensor. The actual self-noise of the Metrozet test sensor is certainly lower at long period. This is due to the fact that the “identical sensor” assumption (splitting the measured incoherent noise equally between the two sensors) is not exactly correct in this case. In fact, the measured incoherent noise is dominated at long periods by the (higher) noise of the PFO reference sensor. Therefore, the actual self-noise of the Metrozet test sensor is lower than is indicated here.

The third plot shows the inter-sensor coherence. It is nearly 1.00000 within the microseismic band. As expected, it drops beyond 40 seconds. This is the point at which the PFO background signal is dropping to a level that is close to the self-noise of the reference sensor.

The final plot shows the relative time series (demeaned and scaled by the scalar responsivities given above). This data has NOT been de-convolved for the frequency response of either sensor. As discussed above, these plots are nearly identical. This is the basis for Metrozet’s claim that frequency response of the two sensors are very close at long period and that the differences in Signal and Self-Noise PSD beyond 40 seconds are due both to higher noise in the Reference sensor and to the very low signal levels at PFO.

In conclusion:

5. The STS1-E300 provides analog performance that matches or exceeds that of the original Factory Electronics box.
6. The calculated self noise of an STS1-E300-equipped sensor is at or below the GSN Noise Model over the a band of 2.5 seconds to 800 seconds).
7. The long period frequency response of a sensor using the STS1-E300 is very close to that of the original sensor.
8. The self-noise of the STS-1 reference sensor is noticeably higher than that of the Metrozet-equipped sensor.

Comparative Plots from pfo Data
Vertical STS-1 Sensors:

PFO Reference STS-1 with Factory Electronics (BLUE)

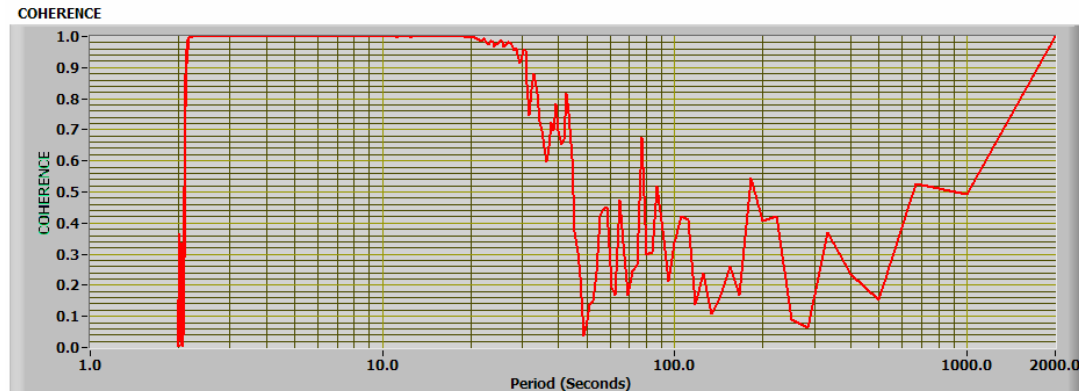
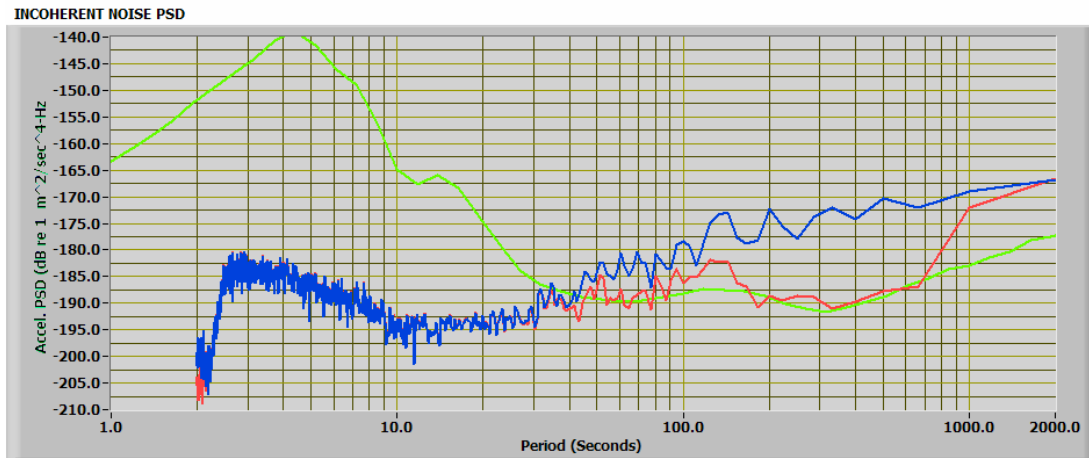
STS-1 with Metrozet STS1-E300 Electronics (RED)

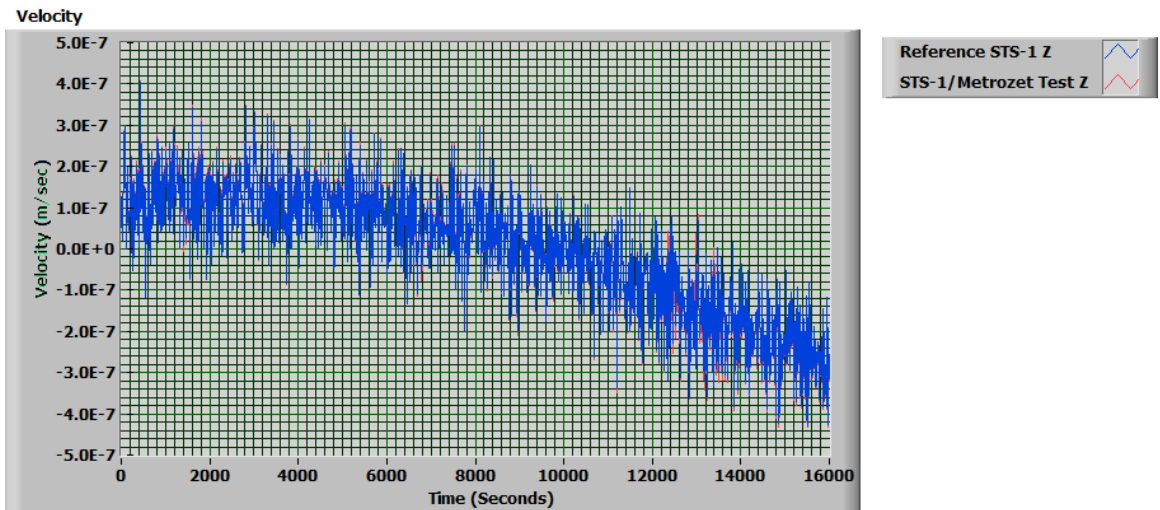
GSN Noise Model (GREEN); after Berger, et al., JGR, 109, B11307 (2004)

Using SAIC Digitizer LH data (1 Hz Output; 0.4 Hz Nyquist)

SIGNAL PSD
INCOHERENT NOISE PSD
COHERENCE

INCOHERENT NOISE PSD Calculated Assuming Identical Sensors





Scaled and de-meaned time series plots for the two sensors (Reference STS-1 in blue, STS-1/Metrozet Test sensor in red) over a 16000 second period. The two sensors have very similar long period response

Appendix C; Analysis of PFO High Frequency Data

High Frequency Response of STS-1 Sensor with Metrozet STS1-E300 Electronics

June 14, 2007

Analysis performed by Metrozet, LLC

Tom VanZandt

To continue with the data analysis for the test of Metrozet's STS1-E300 electronics at PFO, I have analyzed 100 Hz data from both the STS-1/Metrozet Test sensor, and for a co-located STS-2 sensor. The latter has a nominal upper frequency response of 50 Hz. As with the previous analysis, we have empirically matched the scalar amplitude response for the two sensors. The STS-1/Metrozet Test sensor has a response of 4817 V/m/sec. We infer that the STS-2 has a response of 1558 V/m/sec.

The STS-2 is assumed to have a nominal upper corner frequency of 50 Hz, with 0.707 (of critical) damping. This corresponds to a conjugate set of poles at $-222.14 \pm 222.14j$ (rads per second). I have fit the STS-1/Metrozet Test sensor data to that of the STS-2 in order to determine its poles. The analysis involves de-convolving the STS-2 data by its nominal poles (to give "exact" acceleration units to the PSD), and then fitting the poles needed in the de-convolution of the STS-1/Metrozet data, in order for the plots to match

The plots shown below apply a set of conjugate poles at $-60.00 \pm 75.00j$ (rads per second) to the Metrozet data. As can be seen below, this gives very good matching (in both the SIGNAL and INCOHERENT NOISE PSDs) out to about 30 Hz. Above 30 Hz, the inter-sensor coherence has dropped far enough to make the comparison rather meaningless. This is the consequence of low signal-to-noise ratios at high frequency!

To summarize: a pair of conjugate poles of $-60.00 \pm 75.00j$ (rads per second) appears to specify well the high frequency response of the STS-1/Metrozet Z sensor.

Comparative Plots from 100 Hz PFO Data
Vertical Metrozet/STS-1 Sensor and PFO STS-2 Sensor:

PFO Reference STS-2 (BLUE)

STS-1 with Metrozet STS1-E300 Electronics (RED)

GSN Noise Model (GREEN); after Berger, et al., JGR, 109, B11307 (2004)

Using SAIC Digitizer Data (100 Hz Output; 40 Hz Nyquist)

SIGNAL PSD
INCOHERENT NOISE PSD
COHERENCE

INCOHERENT NOISE PSD Calculated Assuming Identical Sensors

